

Photocontrolled Multidirectional Differentiation of Mesenchymal Stem Cells on an Upconversion Substrate

Zhengqing Yan, Hongshuang Qin, Jinsong Ren, and Xiaogang Qu*

Abstract: The effective guidance of mesenchymal stem cell (MSC) differentiation on a substrate by near-infrared (NIR) light is particularly attractive for tissue engineering and regenerative medicine. However, most of current substrates cannot control multidirectional differentiation of MSCs like natural tissues. Herein, a photocontrolled upconversion-based substrate was designed and constructed for guiding multidirectional differentiation of MSCs. The substrate enables MSCs to maintain their stem-cell characteristics due to the anti-adhesive effect of 4-(hydroxymethyl)-3-nitrobenzoic acid modified poly(ethylene glycol) (P1) attached on the upconversion substrate. Upon NIR irradiation, the P1 is released from the substrate by photocleavage. The detachment of P1 can change cell–matrix interactions dynamically. Moreover, MSCs cultured on the upconversion substrate can be specifically induced to differentiate to adipocytes or osteoblasts by adjusting the NIR laser. Our work provides a new way of using NIR-based upconversion substrate to modulate the multidirectional differentiation of MSCs.

As one of the widely studied pluripotent stem cells, mesenchymal stem cells (MSCs) have been considered as the most eligible cells for skeletal tissue engineering and regenerative medicine.^[1] Guiding the differentiation of stem cells into specific cell-types on the matrix efficiently is crucial for stem-cell-based regeneration. Traditionally, growth factors are often used to control stem-cell fate. However, this approach is still facing disappointing clinical outcomes from trials.^[2] There is thus an urgent need to develop alternative strategies to control stem-cell differentiation. Engineering cell-culture matrices is a good way approaching this issue^[3] because the complex signaling pathways of stem cells can be regulated by the physicochemical properties of the extracellular matrix, such as surface composition,^[1a,4] adhesive ligands,^[5] topography,^[6] smoothness/roughness,^[7] and flexibility/rigidity.^[8] To date, some natural materials, such as alginate and hyaluronic acid^[9] and synthetic materials,^[3b,d] have been developed as matrices. Natural materials can provide a bio-

compatible environment. However, the complex composition of natural materials usually makes it difficult to elucidate their corresponding effects on cell differentiation. In contrast, smart artificial interface materials are usually easy to modify with functional biomolecules, which can dynamically switch stem cells from self-renewal to differentiation through a simple chemical microenvironmental change.^[3a] In particular, photo-switched substrates have attracted much attention since they possess the advantages of high spatial and temporal precision and are environmentally friendly.^[5c,10] However, most studies have focused on high-energy UV/Vis light, which limits their further applications in vivo due to the harmful side effects and poor tissue penetration of UV/Vis light. Therefore, it is necessary to develop biocompatible substrates to control cell differentiation dynamically.

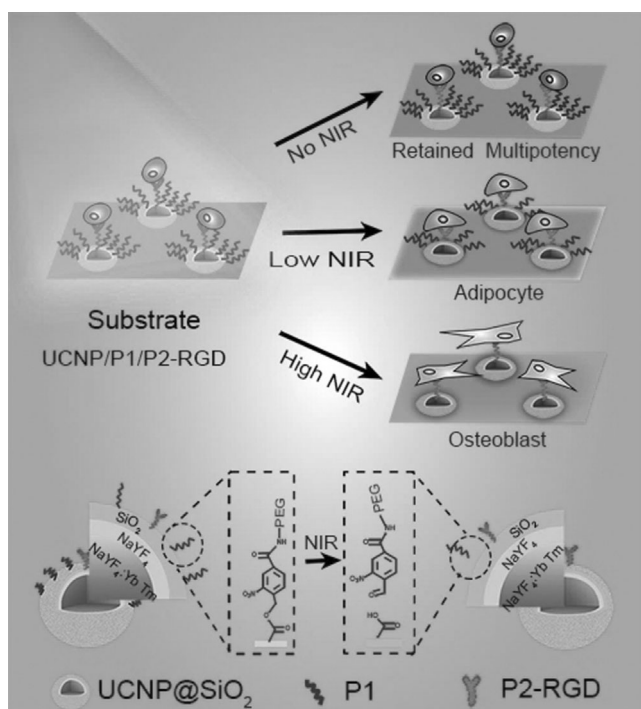
Since lanthanide-doped upconversion nanoparticles (UCNPs) possess the intrinsic properties of absorbing and converting near-infrared (NIR) light into high-energy UV, visible, or NIR irradiation, they have been widely applied in biodetection,^[11] nanomedicines,^[12] and information security.^[13] In our previous studies, UCNPs have been used for on-demand manipulation of cell behaviors, such as cell capture and release^[14] and neurite outgrowth of PC12 cells.^[15] Bian et al. recently reported that UCNPs can be used to trigger the release of small molecules (e.g., kartogenin) and subsequently induce the chondrogenic differentiation of MSCs.^[16] Although promising, none of the reported UCNPs-based materials can modulate the multidirectional differentiation of mesenchymal stem cells like natural tissues. Developing a UCNP-based platform that enables MSCs to be differentiated into diverse cell types is still challenging.

In this work, we designed and constructed a UCNP-based substrate by molecular engineering. The substrate properties can be adjusted by NIR irradiation, which modulates multidirectional differentiation of MSCs. As illustrated in Scheme 1, the substrate (named UCNP/P1/P2-RGD) consists of UCNPs, 4-(hydroxymethyl)-3-nitrobenzoic acid (ONA, a commonly employed photo-cleavage molecule^[17]) modified poly(ethylene glycol) (PEG) (marked as P1) and arginine-glycine-aspartic acid (RGD)-modified PEG (marked as P2). The RGD moieties of P2 on UCNP/P1/P2-RGD can capture MSCs, while the PEG moieties of P1 can block the interaction between MSCs and substrate.^[18] Under NIR laser irradiation, the UCNPs can convert NIR light into UV irradiation. The UV irradiation can control the detachment of P1 and subsequently change cell–matrix interactions. Strong correlations exist between the P1 detachment and the power density of the NIR irradiation. Upon low-power NIR irradiation (0.5 W cm⁻²), MSCs tend to differentiate into adipocytes due to the fact that some P1 start to be released from the

[*] Z. Yan, H. Qin, Prof. J. Ren, Prof. X. Qu
Laboratory of Chemical Biology and
State Key Laboratory of Rare Earth Resource Utilization
Changchun Institute of Applied Chemistry
Chinese Academy of Sciences, Changchun, Jilin 130022 (China)
E-mail: xqu@ciac.ac.cn

Z. Yan
University of Chinese Academy of Sciences
Beijing, 100039 (China)

Supporting information and the ORCID identification number(s) for the author(s) of this article can be found under:
<https://doi.org/10.1002/anie.201803939>



Scheme 1. Schematic illustration of modulating cell–matrix interactions and fate commitment of mesenchymal stem cells (MSCs) by using a UCNP-based substrate.

substrate. Since more P1 are detached from the substrate upon high-power NIR irradiation than that upon low-power NIR irradiation, MSCs display high level of osteogenic differentiation at 6 W cm^{-2} NIR irradiation. This work provides evidence that an upconversion substrate can be used to regulate multidirectional differentiation of MSCs by adjusting NIR laser.

As a starting point for our work, P1 was synthesized according to the procedures in Scheme S1. P1 exhibits an obvious absorption band between 200 and 400 nm (Figure S1 in the Supporting Information), thus suggesting that ONA was included in P1. UCNPs ($\text{NaYF}_4:\text{TmYb}$) that can harvest NIR were utilized as a UV source for photocleavage of P1. The UCNPs were synthesized through thermal decomposition.^[19] Transmission electron microscopy (TEM) images demonstrated that the UCNPs possessed uniform hexagonal shapes with an average diameter of 45 nm (Figure 1a and Figure S2). The high-resolution TEM (HRTEM) images in Figure 1b show that the typical *d*-spacing value was 0.52 nm, thus suggesting a single hexagonal-phase crystal of the UCNPs. To increase the water solubility and biocompatibility, a silica shell was coated onto the UCNPs by using a micro-emulsion method to give UCNP@SiO_2 . The overall size of UCNP@SiO_2 was approximately 75 nm and the thickness of thin silica shells was 15 nm (Figure 1c and Figure S3). Meanwhile, TEM elemental mapping of Si, F, Y, Yb, and Tm further confirmed the formation of UCNP@SiO_2 nanoparticles (Figure 1d). Power X-ray diffraction peaks of UCNP@SiO_2 (Figure S4) were consistent with the standard card No. 28–1192. The obvious UV emission in the upconversion luminescence (UCL) emission spectrum (Figure S5) is attrib-

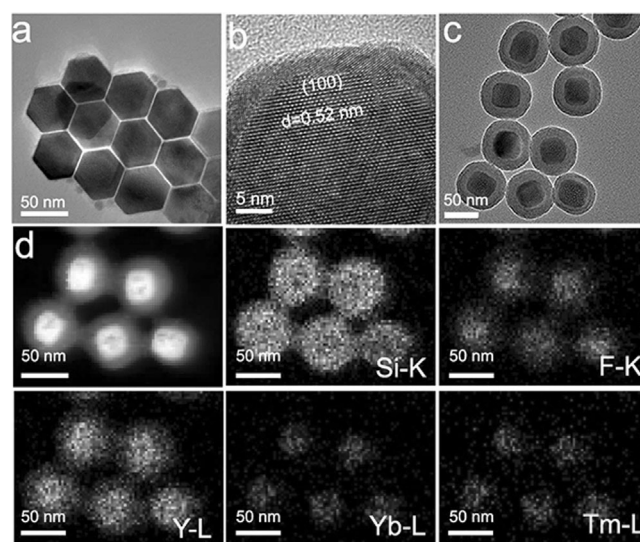


Figure 1. a) TEM and b) HRTEM images of $\text{NaYF}_4:\text{TmYb}$. c) TEM image of UCNP@SiO_2 . d) Dark-field TEM image of UCNP@SiO_2 and its corresponding TEM elemental mappings of Si-K, F-K, Y-L, Yb-L, and Tm-L edge signals.

uted to $^1\text{I}_6 \rightarrow ^3\text{F}_4$ (345 nm) and $^1\text{D}_2 \rightarrow ^3\text{H}_6$ (368 nm) transitions of Tm^{3+} ions,^[20] which could activate photo-cleavage of P1 molecule. When light from an NIR laser traveled through the UCNPs and UCNP@SiO_2 colloidal solutions, purple-blue photoluminescence was also observed (Figure S5, inset). To obtain amino-functionalized nanohybrids ($\text{UCNP@SiO}_2\text{-NH}_2$), the surface of UCNP@SiO_2 was modified with (3-aminopropyl)triethoxysilane. The corresponding modification processes were evaluated by Fourier transform infrared spectra and zeta potential (Figure S6). Next, the substrate UCNP/P1/P2-RGD was prepared according to the procedures shown in Scheme S2. The carboxyl-containing substrate was first modified with $\text{UCNP@SiO}_2\text{-NH}_2$. Then P1 and P2 were introduced onto the surface together (UCNP/P1/P2) through a carbodiimide-mediated wet-chemistry approach. Then, in order to endow the smart substrate with the ability to capture cells, an amino-group-containing RGD was covalently conjugated on the carboxyl motif of P2. The substrate UCNP/P1/P2-RGD was constructed. SEM images showed the surface topography of the substrate (Figure S7a). The absorption spectrum of the substrate in Figure S7b coincided with the absorption spectrum of the photoactive molecule P1, which confirmed that polymer P1 was attached onto surface successfully. Moreover, both the photograph and UCL emission spectroscopy of substrate UCNP/P1/P2-RGD were obtained (Figure S7c). For demonstrating that RGD was added onto the substrate, a cell-capture experiment was carried out. As shown in Figure S7d,e, few cells were attached on the unmodified surface. In contrast, more cells were adherent on the modified surface. Taken together, these results suggest that UCNP/P1/P2-RGD was prepared successfully.

To explore whether an NIR laser could be used to dynamically control P1 detachment from the upconversion substrate, the model dye fluorescein isothiocyanate (FITC)

was covalently modified onto the amino terminus of P1 moieties for visualization. As shown in Figure 2a, after modification, the substrate emitted bright green fluorescence. Then the substrate was immersed in water and treated with low-power or high-power NIR laser. After the substrate was treated with a low-power NIR laser, the fluorescence intensity

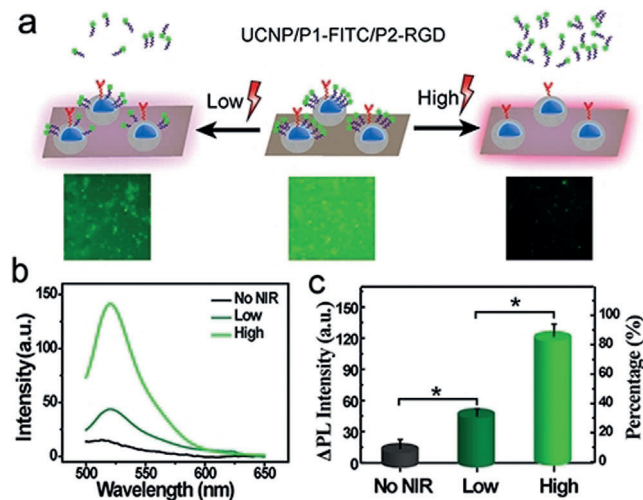


Figure 2. a) Schematic illustration and fluorescence images of substrate (UCNP/P1-FITC/P2-RGD) exposed to no NIR, low-power NIR, or high-power NIR irradiation. b) Fluorescent spectra of solutions of UCNP/P1-FITC/P2-RGD upon exposure to no NIR, low-power NIR, or high-power NIR irradiation. c) Δ PL intensity of solutions and the percentage of P1 detachment. $n = 3$.

dropped slightly. The fluorescence of the substrate decreased sharply upon exposure to high power NIR irradiation. Next, to quantify the percentage of P1 detachment, the fluorescence intensity changes of the surrounding solution upon different power density and time duration were investigated. Figure S8a showed that the fluorescence intensity of the solution, including UCNP/P1-FITC/P2-RGD increased when the power density was increased from 0.5 W cm^{-2} to 6 W cm^{-2} . Above 6 W cm^{-2} , the increase was not significant. So, in our following experiments, 6 W cm^{-2} and 0.5 W cm^{-2} were chosen as high and low power densities, respectively, unless otherwise specified. Negligible changes in fluorescence intensity were detected without NIR irradiation, which confirms that almost no P1 was released from the substrate (Figure S8b). Compared with the fluorescence intensity changes in Figure S8b and S8c, the changes in Figure S8d increased rapidly within 5 min, and then the fluorescence intensity no longer changed after 5 min at 6 W cm^{-2} NIR irradiation, which suggests that most of the P1 was released within 5 min. Therefore, the irradiation time duration was set as 5 min in the following experiments. As shown in Figure 2b,c, about 35% P1 was released from substrate upon 0.5 W cm^{-2} NIR irradiation for 5 min and 90% P1 released upon 6 W cm^{-2} NIR irradiation for 5 min. The successful detachment of P1 upon NIR irradiation provided a possibility for the next step to control the differentiation behavior of MSCs.

Before studying the differentiation behavior of MSCs, we first explored the biocompatibility of UCNP/P1/P2-RGD upon low-power or high-power NIR irradiation. MSCs were cultured on UCNP/P1/P2-RGD and cell viability was assessed with methyl thiazolyl tetrazolium (MTT) assay. As shown in Figure S9, both UCNP/P1/P2-RGD + low power NIR laser and the UCNP/P1/P2-RGD + high power NIR laser had little effect on cell viability under our experimental conditions. Next, in order to explore cell pluripotency after culturing on the smart substrate, the expression of Sox2, Nanog, and Oct4, important genes related to cell pluripotency ("stemness"), were measured by quantitative real-time PCR (qRT-PCR).^[21] The results in Figure 3a showed that the stemness markers

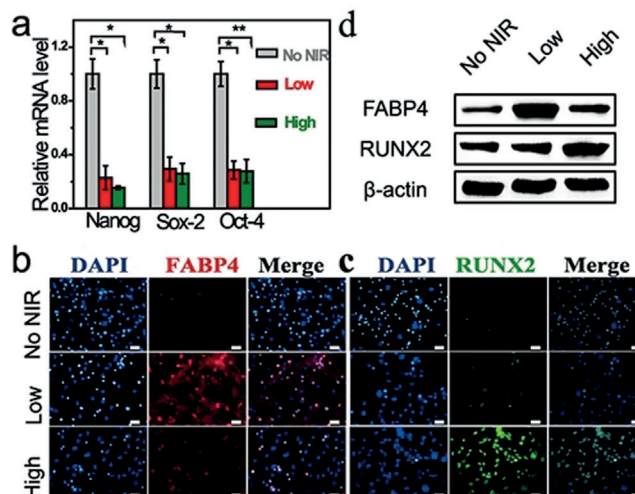


Figure 3. MSCs were cultured on UCNP/P1/P2-RGD with exposure to no NIR, low-power NIR, or high-power NIR irradiation in bipotential differentiation media for 21 days. a) The expression of Sox2, Nanog, and Oct4 ($*p < 0.05$, $n = 3$). b, c) Immunofluorescence imaging of markers for osteogenic (RUNX2, green) and adipogenic (FABP4, red) differentiation. Scale bar: $50 \mu\text{m}$. d) Western blot analysis showing the expression levels of osteogenic (RUNX2) and adipogenic (FABP4) proteins in MSCs.

Sox2, Nanog and Oct4 were positive for MSCs cultured on the smart substrate without NIR exposure. Upon both low-power and high-power NIR irradiation, the expression of Sox2, Nanog, and Oct4 was decreased significantly. This suggests that the designed substrate maintained MSCs pluripotency in the absence of NIR irradiation and the differentiation of MSCs was triggered by P1 detachment in presence of NIR irradiation.

To investigate the differentiation of MSCs cultured on UCNP/P1/P2-RGD with different treatments, oil red O and alizarin red S staining were carried out to measure neutral lipids and calcium deposition respectively. Neutral lipids are recognized as crucial indicators for mature adipocytes and calcium deposition is an important marker for mature osteoblasts. As shown in Figure S10, neither neutral lipids (an adipogenesis marker) nor calcium deposition (an osteogenic marker) was found in MSCs on the substrate in the absence of NIR exposure. With group of low-power NIR irradiation, the MSCs exhibited primarily adipogenic differ-

entiation (staining of neutral lipids) and a very low level of osteogenic differentiation (staining of calcium deposition). Whereas, for the high-power NIR group, the MSCs differentiated into osteoblasts. Next, immunofluorescence and western blot were carried out to further verify differentiation of MSCs. The cells were stained with a cy5-conjugated antibody against the adipogenic marker FABP4 (red fluorescence) and a FITC-conjugated antibody against the osteogenic marker RUNX2 (green fluorescence). A strong red signal was found in cytoplasm and nucleus, thus indicating the emergence of the FABP4 in the low-power NIR group (Figure 3b). However, this adipogenic antigen was not over-expressed when the substrate was treated with high-power NIR irradiation. In addition, strong green fluorescence was observed in the nucleus (Figure 3c), which suggested that RUNX2 was upregulated in MSCs cultured on UCNP/P1/P2-RGD upon high-power NIR irradiation. In contrast, expression of this osteogenic antigen expression was negligible in the low-power NIR group. For the control group without any NIR irradiation, neither red nor green fluorescence appeared. Notably, lots of signals were observed in samples exposure to no NIR or low NIR, which may attributed to the anti-adhesion effects of P1 on UCNP/P1/P2-RGD. Once the substrate was treated with the high-power laser, about 90% of P1 (according to the data in Figure 2c) was detached from the substrate, which could explain why few signals appeared on the substrate. This shows that P1 played a vital role in the cell-matrix interactions. Additionally, the expression of FABP4 and RUNX2 in MSCs were semi-quantified by using Image J software (Figure S11). The mean fluorescence intensity of the red signal (FABP4 expression) in the low-power NIR groups was significantly higher than that in the groups with no NIR irradiation or high-power NIR irradiation. The mean fluorescence intensity of the green signal (RUNX2 expression) in the high-power NIR group was significantly higher than that in the no NIR or low-power NIR groups. Western blot analysis of osteogenic (RUNX2) and adipogenic (FABP4) protein expression in MSCs also showed a similar result (Figure 3d). According to the results discussed above, we concluded that NIR light can be used control cell differentiation effectively. MSCs cultured on the substrate with low-power NIR irradiation tended to differentiate into adipogenic cells, while osteogenic differentiation was favored when the substrate was treated with high-power NIR irradiation.

The relationship between cell morphology and fate were next examined. The morphological changes on the upconversion substrate were explored by phalloidin staining for filamentous actin (F-actin) after different treatments. Figure 4 showed that strong correlations were observed between cell morphology and NIR irradiation. Figure 4a showed that MSCs retained a round shape or spindle fibroblast-like shape without NIR exposure. Upon NIR irradiation, the cells tended to spread on the substrate (Figure 4b and Figure 4c). Moreover, a larger round adipocyte-like shape was observed following low-power NIR irradiation (Figure 4b), and the cells took up polygon shape following high-power NIR irradiation (Figure 4c), which is the typical morphology of osteoblasts. To further study

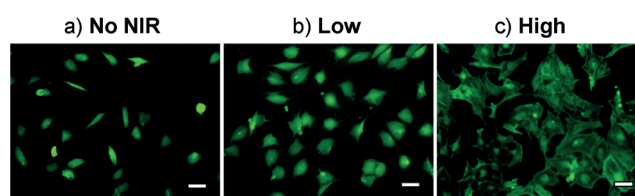


Figure 4. Representative fluorescence microscopy images of cells cultured on UCNP/P1/P2-RGD with exposure to no NIR (a), low-power NIR (b) or, high-power NIR (c) irradiation. The cells were stained for F-actin (green) to show the cell morphology. Scale bar: 50 μm .

whether cell differentiation was modulated by the departure of polymer P1, the light-responsive polymer P1 was substituted with non-light-responsive PEG, marked as UCNP/PEG/P2-RGD. Compared with MSCs on UCNPs/P1/P2-RGD (Figure S12a), MSCs cultured on UCNPs/PEG/P2-RGD (Figure S12b) exhibited low levels of cell differentiation, no matter whether the substrate was treated with NIR irradiation or not. In addition, to investigate the importance of cell contractility to cell differentiation, the cell-contraction inhibitor 2,3-butanedione monoxide was used to treat MSCs cultured on UCNPs/P1/P2-RGD and UCNPs/PEG/P2-RGD. The MSCs on UCNPs/P1/P2-RGD were prone to differentiate to adipogenic cells in the presence of 2,3-butanedione monoxide, despite high-power NIR irradiation (Figure S12c). As for MSCs on UCNPs/PEG/P2-RGD, they still displayed low levels of cell differentiation in the face of 2,3-butanedione monoxide, independent of NIR irradiation. (Figure S12d) These results indicate that changes in cytoskeletal tension play an important role in modulating cell differentiation, which is consistent with previous reports.^[5a,b,6a,c] That is to say, when the polymer P1 are detached from the substrate, the force between cell and substrate would change. Cells can sense the force change^[22] and transduce it into biochemical signals such as β -catenin,^[23] thereby leading to osteogenic and adipogenic differentiation of MSCs.

In summary, we successfully prepared a new photocontrolled upconversion-based substrate. The substrate enables MSCs to maintain their stem-cell properties due to the anti-adhesive effect of P1 attached on the substrate. Upon NIR irradiation, the P1 is released from the substrate by photocleavage, with the level of NIR irradiation controlling the percentage of P1 detachment and subsequently change in cell-matrix interactions. Furthermore, western blot analysis, immunofluorescence, RT-PCR, and oil red O/alizarin red S staining were carried out. The results demonstrate that MSCs tend to differentiate into adipogenic cells under low-power NIR irradiation, whereas osteogenic differentiation is favored under high-power NIR irradiation. Our work provides a new way to modulate multidirectional differentiation of MSCs by using a NIR-based upconversion substrate.

Acknowledgements

Financial support was provided by NSFC (21210002, 21431007, 21533008) and Key Program of Frontier of Sciences, CAS QYZDJ-SSW-SLH052.

Conflict of interest

The authors declare no conflict of interest.

Keywords: cell adhesion · NIR irradiation · photocleavage · tissue engineering · upconversion nanoparticles

- [1] a) P. Rico, H. Mnatsakanyan, M. J. Dalby, M. Salmerón-Sánchez, *Adv. Funct. Mater.* **2016**, *26*, 6563–6573; b) J. Xu, J. Li, S. Lin, T. Wu, H. Huang, K. Zhang, Y. Sun, K. W. K. Yeung, G. Li, L. Bian, *Adv. Funct. Mater.* **2016**, *26*, 2463–2472; c) T. Baudequin, M. Tabrizian, *Adv. Healthcare Mater.* **2017**, 1700734; d) J. A. Kim, H. S. Yun, Y. A. Choi, J. E. Kim, S. Y. Choi, T. G. Kwon, Y. K. Kim, T. Y. Kwon, M. A. Bae, N. J. Kim, Y. C. Bae, H. I. Shin, E. K. Park, *Biomaterials* **2018**, *157*, 51–61; e) Q. L. Ma, L. Fang, N. Jiang, L. Zhang, Y. Wang, Y. M. Zhang, L. H. Chen, *Biomaterials* **2018**, *154*, 234–247; f) Y. Wei, X. Mo, P. Zhang, Y. Li, J. Liao, Y. Li, J. Zhang, C. Ning, S. Wang, X. Deng, L. Jiang, *ACS Nano* **2017**, *11*, 5915–5924; g) S. Zhang, S. J. Chuah, R. C. Lai, J. H. P. Hui, S. K. Lim, W. S. Toh, *Biomaterials* **2018**, *156*, 16–27.
- [2] a) M. Simons, *Circulation* **2002**, *105*, 788–793; b) T. D. Henry, B. H. Annex, G. R. McKendall, M. A. Azrin, J. J. Lopez, F. J. Giordano, P. K. Shah, J. T. Willerson, R. L. Benza, D. S. Berman, C. M. Gibson, A. Bajamonde, A. C. Rundle, J. Fine, E. R. McCluskey, V. Investigators, *Circulation* **2003**, *107*, 1359–1365; c) M. Simons, J. A. Ware, *Nat. Rev. Drug Discovery* **2003**, *2*, 863–871; d) K. Lee, E. A. Silva, D. J. Mooney, *J. R. Soc. Interface* **2011**, *8*, 153–170; e) M. Mahmoudi, S. Bonakdar, M. A. Shokrgozar, H. Aghaverdi, R. Hartmann, A. Pick, G. Witte, W. J. Parak, *ACS Nano* **2013**, *7*, 8379–8384.
- [3] a) E. Dawson, G. Mapili, K. Erickson, S. Taqvi, K. Roy, *Adv. Drug Delivery Rev.* **2008**, *60*, 215–228; b) O. Z. Fisher, A. Khademhosseini, R. Langer, N. A. Peppas, *Acc. Chem. Res.* **2010**, *43*, 419–428; c) S. Shah, P. T. Yin, T. M. Uehara, S. T. Chueng, L. Yang, K. B. Lee, *Adv. Mater.* **2014**, *26*, 3673–3680; d) R. Chen, J. Wang, C. S. Liu, *Adv. Funct. Mater.* **2016**, *26*, 8810–8823; e) Z. Wang, F. Zhang, Z. Wang, Y. Liu, X. Fu, A. Jin, B. C. Yung, W. Chen, J. Fan, X. Yang, G. Niu, X. Chen, *J. Am. Chem. Soc.* **2016**, *138*, 15027–15034; f) A. W. Holle, J. L. Young, K. J. Van Vliet, R. D. Kamm, D. Discher, P. Janmey, J. P. Spatz, T. Saif, *Nano Lett.* **2017**, <https://doi.org/10.1021/acs.nanolett.7b04982>; g) D. S. Wong, J. Li, X. Yan, B. Wang, R. Li, L. Zhang, L. Bian, *Nano Lett.* **2017**, *17*, 1685–1695.
- [4] H. Zhao, O. J. Osborne, S. Lin, Z. Ji, R. Damoiseux, Y. Wang, A. E. Nel, S. Lin, *Small* **2016**, *12*, 4404–4411.
- [5] a) N. Huebsch, P. R. Arany, A. S. Mao, D. Shvartsman, O. A. Ali, S. A. Bencherif, J. Rivera-Feliciano, D. J. Mooney, *Nat. Mater.* **2010**, *9*, 518–526; b) K. Kristopher, A. M. Mrksich, *Angew. Chem. Int. Ed.* **2012**, *51*, 4891–4895; *Angew. Chem.* **2012**, *124*, 4975–4979; c) T. Bai, A. Sinclair, F. Sun, P. Jain, H. C. Hung, P. Zhang, J. R. Ella-Menye, W. Liu, S. Jiang, *Chem. Sci.* **2016**, *7*, 333–338.
- [6] a) M. J. Dalby, N. Gadegaard, R. O. Oreffo, *Nat. Mater.* **2014**, *13*, 558–569; b) T. H. Kim, S. Shah, L. T. Yang, P. T. Yin, M. K. Hossain, B. Conley, J. W. Choi, K. B. Lee, *ACS Nano* **2015**, *9*, 3780–3790; c) C. Yang, F. W. DelRio, H. Ma, A. R. Killaars, L. P. Basta, K. A. Kyburz, K. S. Anseth, *Proc. Natl. Acad. Sci. USA* **2016**, *113*, E4439–E4445.
- [7] A. B. Faia-Torres, S. Guimond-Lischer, M. Rottmar, M. Charnley, T. Goren, K. Maniura-Weber, N. D. Spencer, R. L. Reis, M. Textor, N. M. Neves, *Biomaterials* **2014**, *35*, 9023–9032.
- [8] a) T. Bai, F. Sun, L. Zhang, A. Sinclair, S. Liu, J. R. Ella-Menye, Y. Zheng, S. Jiang, *Angew. Chem. Int. Ed.* **2014**, *53*, 12729–12734; *Angew. Chem.* **2014**, *126*, 12943–12948; b) O. Chaudhuri, L. Gu, D. Klumpers, M. Darnell, S. A. Bencherif, J. C. Weaver, N. Huebsch, H. P. Lee, E. Lippens, G. N. Duda, D. J. Mooney, *Nat. Mater.* **2016**, *15*, 326–334.
- [9] a) S. Gerecht, J. A. Burdick, L. S. Ferreira, S. A. Townsend, R. Langer, G. Vunjak-Novakovic, *Proc. Natl. Acad. Sci. USA* **2007**, *104*, 11298–11303; b) A. Solanki, S. Shah, K. A. Memoli, S. Y. Park, S. Hong, K. B. Lee, *Small* **2010**, *6*, 2509–2513; c) J. Dixon, D. Shah, C. Roger, S. Hall, N. Westond, C. Parmentere, D. McNally, C. Denning, K. Shakesheff, *Proc. Natl. Acad. Sci. USA* **2014**, *111*, 5580–5585; d) P. J. Wrighton, J. R. Klim, B. A. Hernandez, C. H. Koonce, T. J. Kamp, L. L. Kiessling, *Proc. Natl. Acad. Sci. USA* **2014**, *111*, 18126–18131.
- [10] K. Han, W. N. Yin, J. X. Fan, F. Y. Cao, X. Z. Zhang, *ACS Appl. Mater. Interfaces* **2015**, *7*, 23679–23684.
- [11] a) Z. Li, S. Lv, Y. Wang, S. Chen, Z. Liu, *J. Am. Chem. Soc.* **2015**, *137*, 3421–3427; b) J. Peng, W. Xu, C. L. Teoh, S. Han, B. Kim, A. Samanta, J. C. Er, L. Wang, L. Yuan, X. Liu, Y. T. Chang, *J. Am. Chem. Soc.* **2015**, *137*, 2336–2342; c) Q. Su, W. Feng, D. Yang, F. Li, *Acc. Chem. Res.* **2017**, *50*, 32–40; d) Y. Li, J. Tang, L. He, Y. Liu, Y. Liu, C. Chen, Z. Tang, *Adv. Mater.* **2015**, *27*, 4075–4080; e) L. Zhou, R. Wang, C. Yao, X. Li, C. Wang, X. Zhang, C. Xu, A. Zeng, D. Zhao, F. Zhang, *Nat. Commun.* **2015**, *6*, 6938.
- [12] a) J. P. Lai, B. R. Shah, Y. X. Zhang, L. T. Yang, K. B. Lee, *ACS Nano* **2015**, *9*, 5234–5245; b) W. Fan, W. Bu, J. Shi, *Adv. Mater.* **2016**, *28*, 3987–4011; c) X. Ai, C. J. Ho, J. Aw, A. B. Attia, J. Mu, Y. Wang, X. Wang, Y. Wang, X. Liu, H. Chen, M. Gao, X. Chen, E. K. Yeow, G. Liu, M. Olivo, B. Xing, *Nat. Commun.* **2016**, *7*, 10432–10438; d) D. Wang, L. Zhu, J. F. Chen, L. Dai, *Angew. Chem. Int. Ed.* **2016**, *55*, 10795–10799; *Angew. Chem.* **2016**, *128*, 10953–10957.
- [13] J. Lee, B. Yoo, H. Lee, G. D. Cha, H. S. Lee, Y. Cho, S. Y. Kim, H. Seo, W. Lee, D. Son, M. Kang, H. M. Kim, Y. I. Park, T. Hyeon, D. H. Kim, *Adv. Mater.* **2017**, *29*, 3169–3176.
- [14] a) W. Li, J. Wang, J. Ren, X. Qu, *J. Am. Chem. Soc.* **2014**, *136*, 2248–2251; b) W. Li, Z. Chen, L. Zhou, Z. Li, J. Ren, X. Qu, *J. Am. Chem. Soc.* **2015**, *137*, 8199–8205.
- [15] Y. Guan, M. Li, K. Dong, J. Ren, X. Qu, *Small* **2014**, *10*, 3655–3661.
- [16] J. Li, W. Lee, T. Wu, J. Xu, K. Zhang, D. Wong, R. Li, G. Li, L. Bian, *Biomaterials* **2016**, *110*, 1–10.
- [17] a) M. Li, Z. Liu, J. Ren, X. Qu, *Chem. Sci.* **2012**, *3*, 868–873; b) Y. Yang, Q. Shao, R. Deng, C. Wang, X. Teng, K. Cheng, Z. Cheng, L. Huang, Z. Liu, X. Liu, B. Xing, *Angew. Chem. Int. Ed.* **2012**, *51*, 3125–3129; *Angew. Chem.* **2012**, *124*, 3179–3183; c) K. Hwang, P. Wu, T. Kim, L. Lei, S. Tian, Y. Wang, Y. Lu, *Angew. Chem. Int. Ed.* **2014**, *53*, 13798–13802; *Angew. Chem.* **2014**, *126*, 14018–14022.
- [18] a) S. Schilp, A. Rosenhahn, M. E. Pettitt, J. Bowen, M. E. Callow, J. A. Callow, M. Grunze, *Langmuir* **2009**, *25*, 10077–10082; b) R. Peng, X. Yao, J. Ding, *Biomaterials* **2011**, *32*, 8048–8057; c) L. K. Ista, G. P. Lopez, *Langmuir* **2012**, *28*, 12844–12850.
- [19] a) H. S. Qian, H. C. Guo, P. C. Ho, R. Mahendran, Y. Zhang, *Small* **2009**, *5*, 2285–2290; b) Z. Chen, L. Zhou, W. Bing, Z. Zhang, Z. Li, J. Ren, X. Qu, *J. Am. Chem. Soc.* **2014**, *136*, 7498–7504.
- [20] B. Liu, C. Li, P. Yang, Z. Hou, J. Lin, *Adv. Mater.* **2017**, *29*, 1605434.
- [21] a) S. J. Greco, K. Liu, P. Rameshwar, *Stem Cells* **2007**, *25*, 3143–3154; b) M. J. Go, C. Takenaka, H. Ohgushi, *Exp. Cell Res.* **2008**, *314*, 1147–1154; c) E. Pierantozzi, B. Gava, I. Manini, F. Roviello, G. Marotta, M. Chiavarelli, V. Sorrentino, *Stem Cells Dev.* **2011**, *20*, 915–923.

- [22] a) D. E. Discher, P. Janmey, Y. L. Wang, *Science* **2005**, *310*, 1139–1143; b) V. Vogel, M. Sheetz, *Nat. Rev. Mol. Cell Biol.* **2006**, *7*, 265–275; c) B. Geiger, J. P. Spatz, A. D. Bershadsky, *Nat. Rev. Mol. Cell Biol.* **2009**, *10*, 21–33; d) B. D. Cosgrove, K. L. Mui, T. P. Driscoll, S. R. Caliari, K. D. Mehta, R. K. Assoian, J. A. Burdick, R. L. Mauck, *Nat. Mater.* **2016**, *15*, 1297–1306; e) K. Ye, X. Wang, L. Cao, S. Li, Z. Li, L. Yu, J. Ding, *Nano lett.* **2015**, *15*, 4720–4729.
- [23] a) B. Sen, Z. Xie, N. Case, M. Ma, C. Rubin, J. Rubin, *Endocrinology* **2008**, *149*, 6065–6075; b) S. Yamazaki, K. Yamamoto, P. de Lanerolle, M. Harata, *Histochem. Cell Biol.* **2016**, *145*, 389–399.

Manuscript received: April 2, 2018

Version of record online: ■■■■■, ■■■■■

Communications

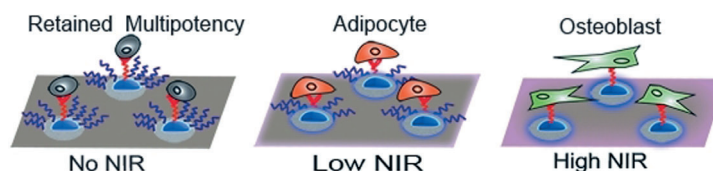


Tissue Engineering

Z. Yan, H. Qin, J. Ren,
X. Qu*



Photocontrolled Multidirectional
Differentiation of Mesenchymal Stem
Cells on an Upconversion Substrate



Leading light: An upconversion-based substrate was designed and constructed for photocontrolled multidirectional differentiation of mesenchymal stem cells (MSCs). The detachment of 4-(hydroxymethyl)-3-nitrobenzoic acid modified

poly(ethylene glycol) moieties on the substrate can be adjusted by near-infrared (NIR) irradiation, which dynamically changes cell–matrix interactions and induces adipogenic or osteogenic differentiation of the MSCs.